J. Mol. Biol. (1984) **179**, 453–467

Torsional Motion of Eosin-labeled F-actin as Detected in the Time-resolved Anisotropy Decay of the Probe in the Sub-millisecond Time Range

HIDEYUKI YOSHIMURA†, TAKUHIRO NISHIO, KOSHIN MIHASHI‡

Department of Physics, Faculty of Science
Nagoya University, Chikusa-ku
Nagoya 464, Japan

KAZUHIKO KINOSITA JR AND AKIRA IKEGAMI

Institute of Physical and Chemical Research
Hirosawa, Wako-shi
Saitama 351, Japan

(Received 31 January 1984, and in revised form 27 June 1984)

The internal motion of F-actin in the time range from 10^{-6} to 10^{-3} second has been explored by measuring the transient absorption anisotropy of eosin-labeled F-actin using laser flash photolysis. The transient absorption anisotropy of eosin–F-actin at 20°C has a component that decays in the submicrosecond time scale to an anisotropy of about 0·3. This anisotropy then decays with a relaxation time of about 450 μs to a residual anisotropy of about 0·1 after 2 ms. When the concentration of eosin–F-actin was varied in the range from 7 to 28 μM, the transient absorption anisotropy curves obtained were almost indistinguishable from each other. These results show that the anisotropy decay arises from internal motion of eosin–F-actin. Analysis of the transient absorption anisotropy curves indicates that the internal motion detected by the decay in anisotropy is primarily a twisting of actin protomers in the F-actin helix; bending of the actin filament makes a minor contribution only to the measured decay. The torsional rigidity calculated from the transient absorption anisotropy is $0{\cdot}2 \times 10^{-17}$ dyn cm^2 at 20°C, which is about an order of magnitude smaller than the flexural rigidity determined from previous studies. Thus, we conclude that F-actin is more flexible in twisting than in bending. The calculated root-mean-square fluctuation of the torsional angle between adjacent actin protomers in the actin helix is about 4° at 20°C. We also found that the torsional rigidity is approximately constant in the temperature range from 5 to ~35°C, and that the binding of phalloidin does not appreciably affect the torsional motion of F-actin.

† Present address: Biometrology Laboratory JEOL Ltd, 1418 Nakagami Akishima, Tokyo 196, Japan.

‡ Author to whom correspondence should be addressed.

0022–2836/84/310453–15 $03.00/0

1. Introduction

At present it is accepted that the free energy of muscle contraction is supplied by hydrolysis of ATP on the "cross-bridges", or myosin heads, that protrude from thick filaments. The key intermediate in this reaction, myosin · ADP · P_i, forms an energized complex with F-actin in the thin filament, and the liberated energy is transformed into the macroscopic work of sliding between thick and thin filaments. In the course of the formation of the energized complex, excitation of the F-actin structure will occur. The movement of F-actin is involved in this process (Oosawa *et al.*, 1973). Our studies have been focused on the flexibility of F-actin in relation to the mechanics of muscle contraction.

Dynamic studies of the flexibility of both F-actin *in vitro* and thin filament *in vivo* have been carried out using various spectroscopic methods (Oosawa, 1980,1983). Depending on the time scale characteristic of the method used, various modes of internal motion of F-actin were found. In the millisecond region, the bending motion of F-actin with a relaxation time of the order of ten milliseconds was detected by measurement of the intensity fluctuations in laser light scattering from F-actin solution (Fujime, 1970). Following this pioneering work, the bending flexibility of F-actin was studied by several other spectroscopic methods (Oosawa, 1980,1983). The flexural rigidity of F-actin obtained in these studies ranges from $1{\cdot}9\times10^{-17}$ dyn cm^2 to $5{\cdot}3\times10^{-17}$ dyn cm^2 (Fujime & Ishiwata, 1971; Yanagida & Oosawa, 1978). Recently, Nagashima & Asakura (1980) and Yanagida *et al.* (1983) succeeded in directly visualizing the overall flexibility of single F-actin filaments in the optical microscope. On the other hand, in the nanosecond region, a rotational correlation time of the order of several hundreds of nanoseconds was obtained in a transient fluorescence anisotropy study of fluorescent labeled F-actin (Wahl *et al.*, 1975; Kawasaki *et al.*, 1975; Ikkai *et al.*, 1979). From these studies, a flexibility of actin protomers in F-actin, arising from some restricted motion in actin protomers, was suggested (Ikkai *et al.*, 1979).

Rotational dynamics of F-actin in the intermediate time range, from microsecond to millisecond, were first reported by Thomas *et al.* (1979), who measured saturation transfer electron paramagnetic resonance spectra using a spin-probe rigidly bound to F-actin. They found that the spin-labeled F-actin undergoes rotational motion that has an effective correlation time of the order of 10^{-4} s, which suggested some restricted intrafilamental motion. However, it was difficult to determine precisely the molecular nature of this motion (Thomas *et al.*, 1979). In order to get more information about the flexibility of F-actin in the microsecond to millisecond time region, we have developed a new approach: measuring, by means of laser flash photolysis, the transient absorption anisotropy of a triplet probe (eosin) bound to F-actin (Mihashi *et al.*, 1983*a*). The principle of transient absorption anisotropy is analogous to the well-known transient fluorescence anisotropy. By virtue of the long lifetime of the triplet probe, usually a few milliseconds (Cherry *et al.*, 1976), the t.a.a.† measurement provides information on the sub-millisecond rotational motions. In our preliminary

† Abbreviations used: t.a.a., transient absorption anisotropy; t.p.a., transient phosphorescence anisotropy; t.f.a., transient fluorescence anisotropy; EIA, eosin-5-iodoacetamide; MalNEt, *N*-ethylmaleimide; e.p.r., electron paramagnetic resonance; S-1, myosin subfragment-1.

experiments on eosin-labeled F-actin at 20°C, the t.a.a. curve showed a relatively slow decay phase, where the apparent decay constant was 450 microseconds, and the residual anisotropy at two milliseconds was ~0·1 (Mihashi *et al.*, 1983*a*). After analysis using the formula of Barkley & Zimm (1979), we found that the t.a.a. can be described very well by the anisotropy decay due to the torsional motion of F-actin. The torsional rigidity calculated was $0{\cdot}19 \times 10^{-17}$ dyn cm^2 at 20°C (Mihashi *et al.*, 1983*b*). This value is much smaller than the flexural rigidity determined for the bending motion (Oosawa, 1980). Recently, Egelman *et al.* (1982) found, by image analysis of electron micrographs of isolated actin filaments, that the F-actin helix is more variable in radial rotation (twist) than in axial displacement. This is very compatible with our results. In the present study, we have more firmly established that the torsional rigidity of F-actin is appreciably smaller than the value predicted from the flexural rigidity for a uniformly elastic thin-rod model. We have also explored the effects of temperature and addition of phalloidin on the torsional motion of F-actin.

2. Materials and Methods

(a) *Reagents*

N-Ethylmaleimide and phalloidin were purchased from Sigma. Eosin-5-iodoacetamide was obtained from Molecular Probes Inc. and it showed a single spot (>97%) on thin-layer chromatography on silica gel plates, using a solution of 40% methanol/60% chloroform (v/v). The EIA was stored at −20°C and dissolved in buffer solution just before the experiment.

(b) *Preparation of EIA–F-actin*

Actin was extracted from acetone-dried powder of rabbit skeletal muscle and purified according to the procedures of Yoshimura & Mihashi (1982). To characterize the labeling of F-actin with EIA, the reactivity of EIA with F-actin and MalNEt-treated F-actin was compared. The latter was prepared by incubation of F-actin with a 1·3 molar excess of MalNEt for 10 h at 4°C, according to Kouyama & Mihashi (1981). F-actin (24 μM) and MalNEt-treated F-actin (24 μM) were incubated with various concentrations of EIA for 6 h at 0°C. The reaction was terminated by addition of 2-mercaptoethanol (1 mM) and the unreacted dye was removed by dialysis. The extent of the reaction was determined by the fluorescence intensity of the labeled F-actin (Fig. 1). MalNEt-treated F-actin, in which a unique cysteine residue, Cys373, was blocked with MalNEt (Elzinga & Collins, 1975), did not show any appreciable labeling with EIA even though there was a 2-fold molar excess of EIA in the solution (Fig. 1). This indicated that the other unblocked cysteine residues did not react with EIA under these solvent conditions.

On the basis of this study of the labeling reaction, EIA–F-actin was prepared as follows. EIA dissolved in 1 mM-$NaHCO_3$ was mixed gently with F-actin solution containing 90 mM-KCl, 2 mM-$MgCl_2$, 0·2 mM-ATP, 1 mM-$NaHCO_3$ at 4°C, with a molar ratio of EIA to actin of 0·7. Five hours after mixing, the reaction was terminated by the addition of 2-mercaptoethanol (1 mM) and the solution was centrifuged for 120 min at 1×10^5 *g*. The pellet of labeled F-actin was dissolved in a solution containing 0·2 mM-ATP, 50 μM-$MgCl_2$, 1 mM-$NaHCO_3$ for depolymerization. A cycle of polymerization–depolymerization was repeated for purification. In the final EIA–F-actin solution, the labeling ratio was 0·2 to ~0·3. A molar extinction of 83,000 M^{-1} cm^{-1} was used for labeled F-actin (Cherry *et al.*, 1976). The protein concentration of the labeled actin was determined using a protein assay kit purchased from Bio-Rad, with $E^{1\%}_{595} = 11{\cdot}0$ cm^{-1}. We found that the molar ratio of EIA to actin decreased with repetition of the polymerization–depolymerization cycle for

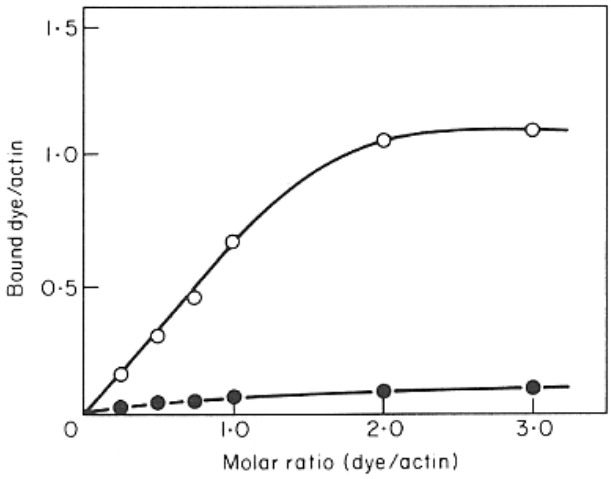

FIG. 1. Fluorometric titration of sulfhydryl groups of F-actin with eosin-5-iodoacetamide. (○) F-actin and (●) MalNEt-treated F-actin were reacted with various concentrations of the dye for 6 h at 0°C. The wavelength of excitation was 530 nm and that of emission was 560 nm. The concentration of both F-actins was 24 μM in 90 mM-KCl, 2 mM-$MgCl_2$, 1 mM-$NaHCO_3$. The concentration of the bound dye was calibrated by absorbance assuming that the molar extinction at 533 nm was 83,000 M^{-1} cm^{-1}.

purification, which suggests that labeled G-actin makes shorter F-actin polymers than unlabeled actin. Measurement of the specific viscosity of EIA–F-actin at different labeling ratios showed a decrease in viscosity corresponding to a reduction in the average length of the F-actin polymers as the extent of labeling was increased (Fig. 2). We found, however, that the critical concentration for polymerization is approximately constant at 0·005 mg/ml, independent of the extent of labeling (Fig. 2).

(c) *Transient absorption anisotropy and transient phosphorescence anisotropy*

Transient absorption anisotropy was measured with a laser flash photolysis apparatus similar to that described by Cherry (1978). The excitation source was a Phase R DL1400 dye laser, which emitted a light pulse of up to 200 mJ of 0·25 μs duration. The 540 nm emission of the dye, Coumarine 540 AF, lies in the absorption band of the eosin label. The emitted light was polarized vertically with a Glan–Taylor prism, which was set in front of the sample cuvette. Transient absorption change in the eosin label after flash excitation arising from ground-state depletion was monitored with continuous light from a 100 W tungsten/halide lamp at 515 nm to avoid detection of prompt fluorescence. Two components of the signal, the vertically polarized one $I_V(t)$ and the horizontally polarized one $I_H(t)$, were separated by a beam-splitting polarizer. The changes in these components, $\Delta I_V(t)$ and $\Delta I_H(t)$, were processed to give both the total absorption change $\Delta A_T(t)$ and the anisotropy $r(t)$, as follows:

$$\Delta A_V(t) = -\log(1+3\Delta I_V(t)/I_0)$$
$$\Delta A_H(t) = -\log(1+3\Delta I_H(t)/I_0)$$
$$\Delta A_T(t) = \Delta A_V(t)+2\Delta A_H(t)$$
$$r(t) = [\Delta A_V(t)-\Delta A_H(t)]/\Delta A_T(t),$$

where I_0 is the total intensity of transmitted monitor light before laser excitation.

The repetition of flash was 2 Hz, and signals from 512 flashes were averaged. The intensity of flash was set so that the absorption change at 20 μs after the laser flash was less than 3% of the total absorbance. The bleaching of the dye was less than 10% after 2048 light flashes. To avoid quenching by oxygen, argon gas was blown over the surface of the

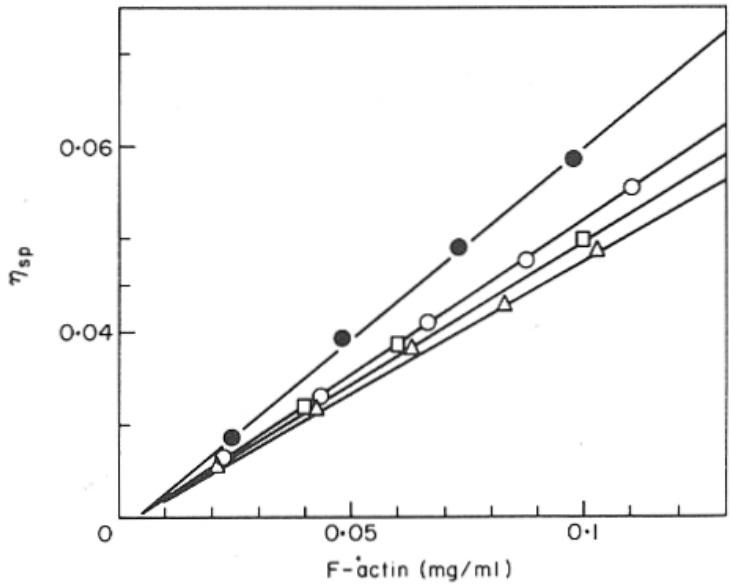

FIG. 2. The concentration dependence of the specific viscosity of F-actin at various ratios of labeling with EIA. The labeling ratio were: (○) 12%, (□) 22%, (△) 27%, and (●) unlabeled. Viscosity was measured with an Ostwald viscometer at 20°C, whose outflow time was 60·5 s for buffer solution. The critical concentration for polymerization is determined by extrapolation to $\eta_{sp} = 0$.

solution, which was gently stirred by the up-and-down motion of a stirrer chip for more than 10 min before each measurement. The decay of the excited state of the labeled probe at 20°C gave an average lifetime of 1·5 ms. Thus, the signal-to-noise ratio of the t.a.a. up to 2 ms after the flash was sufficient for analysis of the anisotropy.

To calculate the torsional motion of EIA–F-actin from the observed t.a.a., curve-fitting was done using the following equations, which describe the anisotropy decay due to torsional motion of a thin flexible rod (Barkley & Zimm, 1979; Allison & Schurr, 1979). The equations were originally developed for the t.f.a. of ethidium bromide intercalated between base-pairs of DNA. Application of the equations to the analysis of t.a.a. is straightforward, since the principle of anisotropy decay is the same in both measurements (Cherry, 1978):

$$r(t) = r_0[A_1 + A_2 \exp(-\sqrt{t/\varphi}) + A_3 \exp(-\sqrt{t/16\varphi})] \quad (1)$$

$$\varphi = (\pi b)^2 \eta C/4(k_B T)^2, \quad (2)$$

where k_B is Boltzmann's constant, T is absolute temperature, η is the viscosity of solvent. The molecular parameters b and C are the radius and the torsional rigidity of thin flexible rod, respectively. A_i values are the function of the angle ω between the absorption dipole moment of the labeled probe and the long axis of the thin rod:

$$A_1 = 0{\cdot}25(2-3\sin^2\omega)^2, \quad A_2 = 0{\cdot}75\sin^4\omega, \quad A_3 = 3\sin^2\omega(1-\sin^2\omega). \quad (3)$$

In the case of t.a.a., the theoretical value of r_0 in eqn (1) is 0·4 (Cherry, 1976). However, we assumed $r_0 = 0{\cdot}32$ on the basis of fluorescence measurement of EIA–F-actin. The static fluorescence anisotropy ($\bar{r}$) of EIA–F-actin at 20°C (excitation at 515 nm and emission at 560 nm) was 0·32, and from the t.f.a. measurement, the anisotropy showed only a slight decay during the lifetime of the fluorescence of the labeled EIA (~2 ns). Since $\bar{r}$ of EIA–acetyl-cysteine in 99% glycerol at 20°C was 0·37, we concluded that the r_0 value of EIA–F-actin was reduced by rapid rotation of the dye at the binding site in the sub-nanosecond time range, which is independent of the motion of protein. Thus, r_0 of the t.a.a. can be approximated using the static fluorescence anisotropy, i.e. 0·32. In a highly viscous solvent (EIA–acetyl-cysteine in 99% glycerol at −20°C), we got a value of $r_0 = 0{\cdot}39$ by t.a.a.

Transient phosphorescence anisotropy of EIA–F-actin was measured using the same apparatus as for t.a.a., with appropriate modification, as follows. A pair of polarizers

(Polaroid HNP'B) and mirrors were set at 2 sides of the sample cuvette at right-angles to the incident laser beam of excitation. The phosphorescence observed through each pair of polarizers and mirrors was introduced to photomultipliers (Hamamatsu TV R1333X). In front of the photomultipliers, filters (SC60 and SC66 × 2 from Fuji Film Co., cut-off <660 nm) were placed to cut prompt fluorescence. The photomultipliers were gated to avoid detection of prompt fluorescence. The data from t.a.a. and t.p.a. were analyzed by a least-squares method using a DEC microcomputer LSI-11/2. Details of the measurement of t.a.a. and t.p.a. will be given elsewhere by Kinosita & Ikegami.

(d) *Transient and static fluorescence measurements*

Both time-resolved and static fluorescence were measured with a single photon-counting apparatus described previously (Kinosita *et al.*, 1981).

(e) *Simulation of the t.a.a. curve*

Simulation of the theoretical curve of t.a.a. was carried out using the facilities of the Nagoya University Computer Center.

3. Results

(a) *Characterization of the t.a.a. of EIA–F-actin*

(i) *The main features of the t.a.a. of EIA–F-actin*

The t.a.a. of EIA–F-actin (14 μM at 20°C) showed that, after a very rapid decay in the initial several tens of microseconds, there followed a relatively slow decay in the first several hundreds of microseconds (Figs 3 and 4). The apparent relaxation time of this phase was 450 microseconds (Mihashi *et al.*, 1983*a*). After this phase, the decay became so slow that the anisotropy could be approximated by a constant value of 0·1 at two milliseconds (Mihashi *et al.*, 1983*b*). The existence of a large residual anisotropy suggests that the rotational motion underlying the t.a.a. is a very strongly restricted internal motion, such as twisting and bending of the EIA–F-actin. Another possible explanation for the t.a.a. is related to the length distribution of EIA–F-actin. Since F-actin in solution usually has a broad length distribution (Oosawa & Asakura, 1975), overall rotation of short EIA–F-actin polymers may contribute to the slow decay phase of t.a.a. and the relative immobility of long EIA–F-actin may give a large residual anisotropy at two milliseconds. If F-actin is represented as a uniformly elastic thin filament, a measure of the flexibility is given by the persistence length, which is 6 to ~17 micrometers for F-actin at room temperature (Fujime, 1970; Oosawa, 1980). F-actin that is substantially shorter than the persistence length should behave as a rigid rod, while F-actin that is longer than the persistence length should behave as a flexible thin filament. Therefore, in order to distinguish between these possibilities, the contribution of a short EIA–F-actin was examined in the two following ways. First, t.a.a. was measured at various concentrations of EIA–F-actin (7 μM to 28 μM) at which the fraction of short EIA–F-actin decreased with increasing concentration. Second, assuming EIA–F-actin to be a rigid thin rod with a broad length distribution, a simulation was

done for t.a.a. decay due to the overall rotation of EIA–F-actin and the calculated t.a.a. was compared with the experimental curve.

(ii) *The t.a.a. of EIA–F-actin at 28 μM to 7 μM at 20°C*

According to the thermodynamic analysis of polymerization of actin (Oosawa & Asakura, 1975), the fraction of short F-actin is reduced by increasing the concentration of actin. Therefore, if the overall rotation of short EIA–F-actin contributed significantly to the decay of t.a.a., the anisotropy would increase at higher concentrations. Inversely, at lower concentrations, the anisotropy would be reduced. We found, however, that the t.a.a. curves at 28 μM and 10 μM were indistinguishable from that at 14 μM (Fig. 3). Even at 7 μM, the observed t.a.a. was quite similar to that at 14 μM (Mihashi *et al.*, 1983*b*). Thus the t.a.a. is independent of the length distribution, at least in the range from 7 μM to 28 μM-EIA–F-actin. Therefore, the decay of the t.a.a. must arise from the internal motion of EIA–F-actin, irrespective of the polymer length (Mihashi *et al.*, 1983*b*).

(iii) *Simulation of t.a.a. decay by the overall rotation of a rigid rod of known length distribution*

Calculation of the expected t.a.a. for the length distribution of F-actin polymers confirms that the observed decay cannot be accounted for by overall rotation of the shorter rods. t.a.a. decay was simulated by assuming that EIA–F-actin is a rigid thin rod to which eosin is specifically attached, with a fixed angle for the absorption dipole moment relative to the long axis of the rod. In the simulation the distribution of the length of the EIA–F-actin in a 14 μM solution was

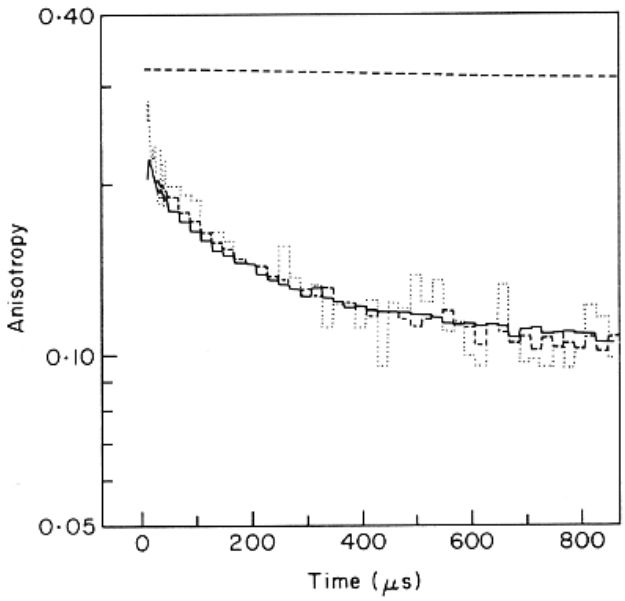

FIG. 3. The transient absorption anisotropy of EIA–F-actin at 20°C. The concentrations of EIA–F-actin were (——) 28 μM, (– – –) 14 μM and (·····) 10 μM. The solution contained 90 mM-KCl, 2 mM-$MgCl_2$, 0·1 mM-$CaCl_2$, 20 mM-Tris-acetate (pH 7·6). The upper broken line is the simulated curve of a rigid thin rod model with a polymeric length distribution (see Appendix).

calculated according to Oosawa (1970), using the value of the thermodynamic parameters obtained in the study of actin polymerization. The contribution of the overall rotation of these rigid rods to the t.a.a. was then summed to give the resultant decay curve. (Details of the calculation are given in the Appendix.) We see in Figure 3 that the anisotropy decay of the simulated curve of t.a.a. in the millisecond time range is less than 10% of the initial anisotropy. Thus, the experimental curve cannot possibly be explained by the overall rotation of EIA–F-actin. The overall rotation of short EIA–F-actin only makes a minor contribution to the t.a.a.

(iv) *Analysis of the observed t.a.a. in terms of the torsional motion of EIA–F-actin*

Since F-actin has a helical structure, the torsional motion of actin protomers around the helical axis, among possible internal motions of F-actin, will most probably be detected by the t.a.a. in the time range from microseconds to milliseconds (Oosawa, 1980). Therefore, the t.a.a. of EIA–F-actin was analyzed according to the theory of anisotropy decay due to torsional motion (Barkley & Zimm, 1979; Allison & Schurr, 1979). In order to apply equations (1), (2) and (3), EIA–F-actin was assumed to be a thin flexible rod of radius $b = 40$ Å. The torsional rigidity C and the angle ω between the absorption dipole and the F-actin helix axis were taken as adjustable parameters. The best fit for the t.a.a. of EIA–F-actin at 14 μM and 20°C was obtained using values for $C = 0{\cdot}18 \times 10^{-17}$ dyn cm^2 and $\omega = 32{\cdot}8°$. The fitting was satisfactory over the whole range of t.a.a. up to two milliseconds (Fig. 4), indicating that the major contribution to the anisotropy decay comes from the torsional motion (Mihashi *et al.*, 1983*b*).

(b) *Temperature dependence of the torsional rigidity of EIA–F-actin*

Equation (2), which was used in the above analysis, requires that the torsional decay constant, φ, must be linearly related to $\eta/(k_B T)^2$ in the temperature range at which the molecular parameters are constant. If any conformational change occurred in EIA–F-actin at any temperature, departure from the linear relation would be observed. To examine this point, the values of the decay constant, φ, measured in the range from 5°C to 35°C, were plotted as a function of $\eta/(k_B T)^2$ in Figure 5. The linear regression of the plot gives a slope equal to $9{\cdot}2 \times 10^{-31}$ dyn cm^4. The scatter of the points relative to this line is within $\pm 15\%$, which suggests that no significant conformational change occurs in this temperature range. The basic helical structure of EIA–F-actin is stable, though the torsional fluctuation is enhanced with increasing temperatute. If we take $b = 40$ Å, the slope is equal to $0{\cdot}23(\pm 0{\cdot}03) \times 10^{-17}$ dyn cm^2. The angle ω, calculated independently from the data at each temperature, remained within $\pm 3°$ of the average, 33°.

(c) *Transient phosphorescence anisotropy of EIA–F-actin*

While the t.a.a. at 20°C was independent of the concentration of EIA–F-actin within the range from 28 μM to 7 μM, as described above, it is possible that a

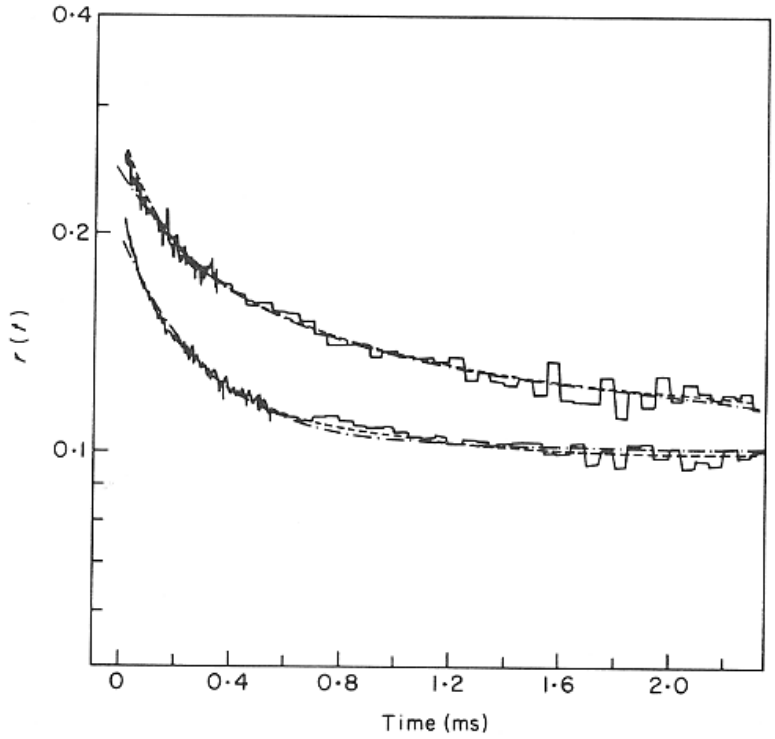

FIG. 4. Temperature dependence of the t.a.a. of EIA–F-actin 14 μM. The unbroken lines are experimental anisotropy decay at 20°C (lower curve) and at 5°C (upper curve). The broken lines are calculated curves using torsional functions (eqn (1)) and chained lines are calculated using exponential functions (2 components). We got a better fit to the experimental data using the torsional functions than the exponential one, especially at the initial decay of the data. The solvent conditions were the same as for Fig. 3.

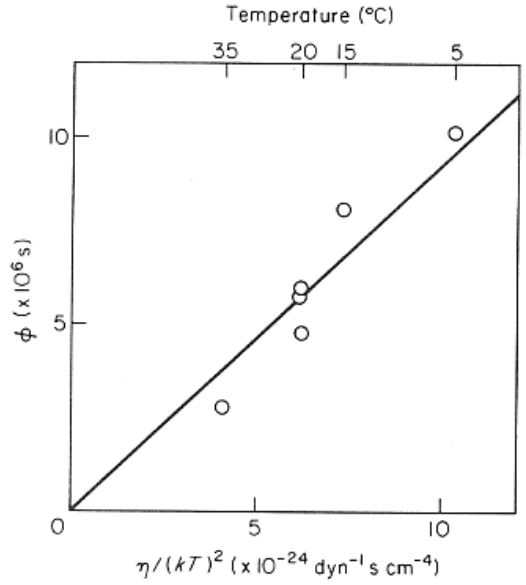

FIG. 5. Temperature dependence of the anisotropy decay constant φ (eqn (2)). The decay constants, φ, obtained from t.a.a. at various temperatures were plotted as a function of $\eta/(k_B T)^2$ according to eqn (2). The straight line is the linear regression of the plot.

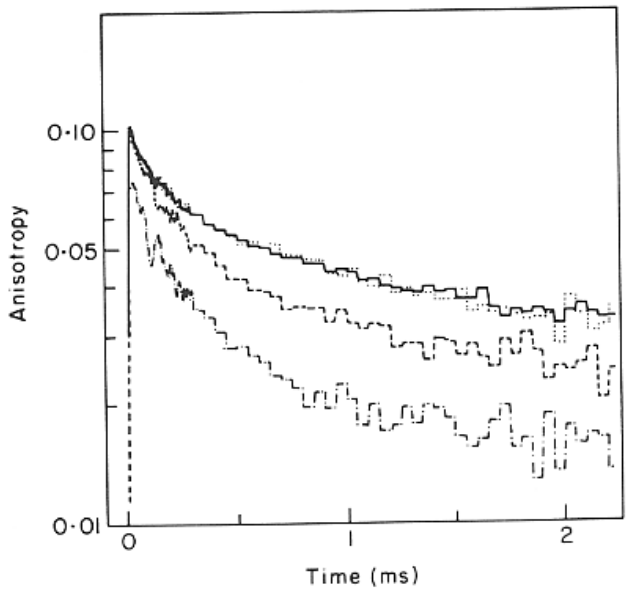

FIG. 6. The transient phosphorescence anisotropy of EIA–F-actin at 20°C. The concentrations of EIA–F-actin were (——) 23 μM. (· · · · ·) 14 μM. (— · —) 1·4 μM. (— — —) 1·4 μM, plus 4·2 μM-phalloidin. The solvent conditions were the same as for Fig. 3.

further reduction in the concentration could affect the t.a.a. Below 5 μM, however, the signal was so weak that significant measurement of the t.a.a. could not be obtained. Then the transient phosphorescence anisotropy of EIA–F-actin was measured, which gave a higher sensitivity than t.a.a. The results were compared for various concentration of EIA–F-actin. As seen in Figure 6, the t.p.a. of EIA–F-actin at 1·4 μM was appreciably lower than that at 14 μM; the fraction of rapidly decaying component increased by lowering the concentration of EIA–F-actin, and the initial anisotropy was also reduced. These changes are due to the increase in the fractions of monomer and short EIA–F-actin. On the other hand, the t.p.a. of EIA–F-actin at 23 μM was essentially identical to that at 14 μM (Fig. 6). Thus t.a.a. and t.p.a. gave essentially the same information on the internal motion of EIA–F-actin, though the initial anisotropy (r_0) is lower in t.p.a. than t.a.a. The difference in r_0 between t.p.a. and t.a.a. is due to the difference in the dipole moments detected in each measurement (Jovin *et al.*, 1981).

(d) *Effect of phalloidin*

Phalloidin, a toxic cyclic peptide extracted from the green deathcap toadstool *Amanita phalloides*, is known to accelerate polymerization of actin and stabilize F-actin against depolymerization by potassium iodide (Dancker *et al.*, 1975). The presence of 4·2 μM-phalloidin with 1·4 μM-EIA–F-actin caused an upward shift in the t.p.a. (Fig. 6), indicating that the fraction of very short EIA–F-actin or monomers decreased. At an EIA–F-actin concentration of 14 μM, addition of phalloidin (55 μM) did not significantly affect the t.p.a. (data not shown). This means that the torsional rigidity of EIA–F-actin is not altered by the binding of phalloidin in spite of the stabilization effect on F-actin.

4. Discussion

(a) *Anisotropic elasticity of F-actin*

According to the principle of t.a.a., anisotropy decay is sensitive to the amplitude of the angular diffusion of the absorption dipole moment of the labeled probe during the lifetime of the triplet state, whether the motion is twisting or bending (Barkley & Zimm, 1979). We found that the t.a.a. of EIA–F-actin at 20°C fits very well with the anisotropy decay calculated for torsional motion only. It appears, therefore, that EIA–F-actin behaves as a torsionally flexible thin rod. Analysis of the t.a.a. showed that the absorption dipole moment of the labeled eosin, ω, assumes an angle of $\sim 33°$ with respect to the long axis of F-actin. At this value of the angle, both torsional and bending motion would be almost equally detectable in the t.a.a. if the torsional rigidity were of the same order of magnitude as the flexural rigidity. In fact, the torsional rigidity is very much smaller than the flexural rigidity. In order to estimate the extent of the contribution of bending motion to the t.a.a., we compared two simulated curves of t.a.a. in which bending motion was either taken into consideration or not. In the simulations, previously reported values for flexural rigidity (Oosawa, 1980) were used: the highest was $5{\cdot}3 \times 10^{-17}$ dyn cm^2 (Yanagida & Oosawa, 1978) and the lowest was $1{\cdot}9 \times 10^{-17}$ dyn cm^2 (Fujime & Ishiwata, 1971). From these calculations, we found that the correction in the value of the torsional rigidity is, at the most, an increase of about 20% using the lowest value for the flexural rigidity (Table 1). Very recently, it was pointed out by Schurr (1984) and Shibata *et al.* (1984) that the Barkley–Zimm formulation overestimates the contribution of bending motion to anisotropy decay. Therefore, it is likely that the necessary correction for bending motion is less than 20%. Thus, the torsional rigidity must be at least seven times smaller than the flexural rigidity.

The classical theory of elasticity predicts that, for a thin flexible rod composed of homogeneous isotropic material, the torsional rigidity (C) and the flexural rigidity (EI) are related in the form (Barkley & Zimm, 1979):

$$C = EI/(1+\sigma),$$

where σ (Poisson's ratio) is about 0·5 (Landau & Lifshiz, 1970). The result given in Table 1 indicates that Poisson's ratio for EIA–F-actin must be at least 11 times

TABLE 1

Torsional rigidity of EIA–F-actin at 20°C (in 10^{-17} dyn cm^2)

Radius of F-actin (assumed)	40 Å†		45 Å‡		50 Å§	
Torsional rigidity (without correction)	0·23		0·18		0·15	
Torsional rigidity (with correction)	0·28	0·25	0·22	0·19	0·18	0·15
Flexural rigidity (used for correction)	1·9‖	5·3¶	1·9‖	5·3¶	1·9‖	5·3¶
(Flexural rigidity)/(torsional rigidity)	6·8	20	8·6	27	11	34
$(\Delta\gamma)_{r.m.s.}$ (°)	3·6	3·8	4·1	4·4	4·5	4·9

† Wakabayashi *et al.* (1975); ‡ Egelman *et al.* (1982); § Tajima *et al.* (1983); ‖ Fujime & Ishiwata (1971); ¶ Yanagida & Oosawa (1978).

larger than the value for a uniform rod. Therefore, EIA–F-actin is not isotropically flexible, but is more flexible in twisting than in bending motion (Mihashi *et al.*, 1983*b*). This is reasonable because F-actin consists of a helical array of promoters that is not uniform along the axis (Hanson & Lowy, 1963). The nature of the change in intersubunit coupling required for twisting will be different from the change required for bending. Macroscopic flexibilities (torsional and flexural rigidities) are then determined by the helical distribution of these microscopic elasticities (Oosawa, 1977).

(b) *Fluctuation of the torsion angle in F-actin*

The present dynamic study of EIA–F-actin in the sub-millisecond time range gives a quantitative description of thermal fluctuation of the basic helical structure of F-actin. An important parameter obtained from the torsional rigidity is the equilibrium fluctuation of the torsional angle of actin protomers in F-actin. The fluctuation of the helical twist angle between the adjacent protomers, $\Delta\gamma$, is related to the torsional rigidity in the following way (Barkley & Zimm, 1979):

$$C\langle\Delta\gamma^2\rangle/2d = k_B T/2,$$

where d is the axial displacement of 27·3 Å per protomer along the helical axis. Solving the equation for the root-mean-square fluctuation, $(\Delta\gamma)_{r.m.s.} = \sqrt{\langle\Delta\gamma^2\rangle}$, we find that $(\Delta\gamma)_{r.m.s.}$ is equal to 4·3° for $C = 0{\cdot}2 \times 10^{-17}$ dyn cm^2 at 20°C (Table 1).

The basic helical parameters of F-actin have been determined from the low-angle X-ray diffraction measurements on muscle fibers or F-actin gels, on the one hand (Vibert *et al.*, 1972; Tajima *et al.*, 1983), and from image analysis of electron micrographs of F-actin paracrystals, on the other (O'Brien *et al.*, 1975; Moore *et al.*, 1970). It should be pointed out that in the image analysis, F-actin paracrystals, in which F-actin is packed side-by-side in an axial register, have been used extensively instead of an isolated single F-actin filament. This is primarily because isolated F-actin filaments tend to be flexible and good micrographs of individual straight F-actin, which would be suitable for image analysis, are rarely obtained (Squire, 1981). Hanson (1967) first noted significant disorder in F-actin helices, from electron micrographs of isolated filaments that showed considerable variation in distance between cross-overs of the two-start helical strands. Disorder in the F-actin helix has been recently analyzed by Egelman *et al.* (1982,1983) by digitized image-processing of electron micrographs. By statistical comparison, they found a much larger fluctuation of twist angle between protomers in isolated F-actin filaments than in Mg^{2+} paracrystals. This picture of the variable twist of the F-actin helix, based on statistical analysis of static images, is very compatible with the dynamic picture of F-actin revealed in the present study. The torsional fluctuation of about 10° in the twist angle between protomers found by image analysis of actin helices (Egelman *et al.*, 1983) is substantially larger than the value of 4·3° found in our study. This may be simply due to the different experimental conditions; our measurements were done on F-actin in thermal equilibrium in solution, while the electron micrographs were

taken after dehydration and staining of F-actin on a grid, which may additionally distort the torsionally flexible helices.

(c) *The effect of myosin head and regulatory proteins*

In the electron paramagnetic resonance study of spin-labeled F-actin, Thomas *et al.* (1979) concluded that rotational motion occurs within F-actin on a scale larger than the immediate environment of the label but smaller than an entire filament. The site of the spin label is probably the same as that of the EIA label in the present t.a.a. study. The rotational correlation time of the spin probe is within the range of the rotational correlation time found from the t.a.a. (Mihashi *et al.*, 1983*a*). Therefore, although Thomas *et al.* were uncertain how to assign the mode of rotation, it is likely that both the e.p.r. and t.a.a. measurements detected the same internal motion of F-actin. In the present study, we have confirmed that torsional motion is dominant.

A significant immobilization of F-actin by the binding of heavy meromyosin or subfragment-1 was observed in the e.p.r. study (Thomas *et al.*, 1979). Correspondingly, a preliminary study of the t.a.a. of EIA–F-actin in the presence of S-1 showed that the residual anisotropy at two milliseconds increases appreciably up to about 0·2 (Yoshimura, unpublished result). The effect showed saturation at a very low molar ratio of S-1 to actin (about 0·05), suggesting that the effect of S-1 binding to an actin protomer spreads over to neighboring actin protomers that are not in direct contact with the myosin head. This is similar to the co-operative effects found in the e.p.r. study (Thomas *et al.*, 1979) and other studies (Oosawa *et al.*, 1973; Miki *et al.*, 1982), which may be related to the co-operative binding of S-1 to F-actin found in a recent study (Yoshimura & Mihashi, 1982). We have also found distinct effects of tropomyosin and troponin on the t.a.a. of EIA–F-actin (Mihashi *et al.*, 1983*b*). Thus it is possible that tropomyosin and troponin together with Ca^{2+} regulate the function of F-actin by modulating the internal rotational motion of F-actin.

APPENDIX

Simulation of the Transient Absorption Anisotropy curve of the Overall Rotational Motion of a Rigid Thin Rod with a Polymeric Length Distribution

TAKUHIRO NISHIO, HIDEYUKI YOSHIMURA AND KOSHIN MIHASHI

The t.a.a. due to the overall rotational motion (end-over-end tumbling and spinning) of a rigid rod whose length and radius are L and b, respectively, is described by the following relation (Rigler & Ehrenberg, 1973):

$$r_L(t) = r_0[A_1 \exp(-t(6D_{2,L})) + A_2 \exp(-t(4D_{1,L}+2D_{2,L})) + A_3 \exp(-t(D_{1,L}+5D_{2,L}))], \quad \text{(A1)}$$

where A_i values are given in equation (3) in the main text. $r_0 = 0{\cdot}32$ and $\omega = 32^c$ were used as described in the main text. $D_{1,L}$ and $D_{2,L}$ are the rotational diffusion constants of the rod around the long and the transverse axis of the rod, respectively (Broersma, 1960):

$$D_{1,L} = k_B T/4\pi\eta b^2 L \tag{A2}$$

$$D_{2,L} = (3k_B T/\pi\eta L^3)[\ln (L/b) - 1{\cdot}57 + 7(1/\ln (L/b) - 0{\cdot}28)^2]. \tag{A3}$$

To generate the theoretical curve of t.a.a., $r_L(t)$ in equation (A1) is summed with respect to the length distribution of F-actin as follows.

According to the thermodynamic theory of polymerization of actin (Oosawa & Asakura, 1975), the concentration of helical i-mer of actin C_{ih} is given as:

$$C_{ih} = \alpha K_h^{-1}(K_h C_1)^i. \tag{A4}$$

where $\alpha = (K/K_h)^2 \exp(-\Delta F^*/k_B T)$. K_h and K are the binding constants of the addition of actin monomer to the helical and linear polymers, respectively. ΔF^* is the excess free energy necessary for deformation of a linear trimer to form a helical trimer. C_1 is the concentration of actin monomers under the experimental conditions. According to Oosawa & Asakura (1975), we took $K_h = 10^7\ \text{M}^{-1}$, $K = 10^6\ \text{M}^{-1}$ and $F^* = +5$ kcal/mol. Finally, the anisotropy of i-mer $r_i(t)$ was summed to give the theoretical curve of the anisotropy decay $r(t)$:

$$r(t) = \frac{\sum_i i\alpha K_h^{-1}(K_h C_1)^i r_{L_i}(t)}{\sum_i i\alpha K_h^{-1}(K_h C_1)^i}. \tag{A5}$$

In this calculation, the length of i-mer F-actin was given as $L_i = 54{\cdot}6 \times i/2$ Å, and $b = 40$ Å is assumed. The theoretical curve thus obtained for EIA–F-actin (14 μM at 20°C) is shown in Figure 3. The simulated curve does not explain the observed decay at all, indicating that the observed decay is associated with internal motion of EIA–F-actin.

The authors are indebted to Professor F. Oosawa for his continuing interest and stimulating discussion on the present study. They thank Dr D. L. D. Casper for his help with this manuscript.

REFERENCES

Allison, S. A. & Schurr, J. M. (1979). *Chem. Phys.* **41**, 35–59.
Barkley, M. D. & Zimm, B. H. (1979). *J. Chem. Phys.* **70**, 2991–3007.
Broersma, S. (1960). *J. Chem. Phys.* **32**, 1626–1635.
Cherry, R. J. (1978). *Methods Enzymol.* **54**, 47–61.
Cherry, R. J., Cogoli, A., Oppliger, M., Schneider, G. & Semenza, G. (1976). *Biochemistry*, **15**, 3653–3656.
Dancker, P., Löw, I., Hasselbach, W. & Wieland, Th. (1975). *Biochim. Biophys. Acta*, **400**, 407–414.
Egelman, E. H., Francis, N. & DeRosier, D. J. (1982). *Nature (London)*, **298**, 131–135.
Egelman, E. H., Francis, N. & DeRosier, D. J. (1983). *J. Mol. Biol.* **166**, 605–623.
Elzinga, M. & Collins, J. H. (1975). *J. Biol. Chem.* **250**, 5897–5905.
Fujime, S. (1970). *J. Phys. Soc., Japan*, **29**, 751–759.

Fujime, S. & Ishiwata, S. (1971). *J. Mol. Biol.* **62**, 251–265.
Hanson, J. (1967). *Nature (London)*, **213**, 353–356.
Hanson, J. & Lowy, J. (1963). *J. Mol. Biol.* **6**, 46–60.
Ikkai, Y., Wahl, Ph. & Auchet, J. C. (1979). *Eur. J. Biochem.* **93**, 397–408.
Jovin, T. M., Bartholdi, M., Vaz, W. L. C. & Austin, R. H. (1981). *Ann. N.Y. Acad. Sci.* **366**, 176–196.
Kawasaki, Y., Mihashi, K., Tanaka, H. & Ohnuma, H. (1976). *Biochim. Biophys. Acta*, **446**, 166–178.
Kinosita, K. Jr, Kataoka, R., Kimura, Y., Gotoh, O. & Ikegami, A. (1981). *Biochemistry*, **20**, 4270–4277.
Kouyama, T. & Mihashi, K. (1981). *Eur. J. Biochem.* **114**, 33–38.
Landau, L. D. & Lifshitz, E. M. (1970). *Theory of Elasticity*, pp. 13–14. Pergamon Press, Oxford, New York, Toronto, Sydney, Paris, Frankfurt.
Mihashi, K., Yoshimura, H. & Nishio, T. (1983*a*). In *Actin: Structure and Function in Muscle & Non-muscle Cells* (dos Remedios & Barden, eds), pp. 81–88. Academic Press, Australia.
Mihashi, K., Yoshimura, H., Nishio, T., Ikegami, A. & Kinosita, K. Jr (1983*b*). *J. Biochem.* **93**, 1705–1707.
Miki, M., Wahl, P. & Auchet, J.-C. (1982). *Biochemistry*, **21**, 3661–3665.
Moore, P. B., Huxley, H. E. & DeRosier, D. J. (1970). *J. Mol. Biol.* **50**, 279–292.
Nagashima, H. & Asakura, S. (1980). *J. Mol. Biol.* **136**, 169–182.
O'Brien, E. J., Gillis, J. M. & Couch, J. (1975). *J. Mol. Biol.* **99**, 461–475.
Oosawa, F. (1970). *J. Theoret. Biol.* **27**, 69–86.
Oosawa, F. (1977). *Biorheology*, **14**, 11–19.
Oosawa, F. (1980). *Biophys. Chem.* **11**, 443–446.
Oosawa, F. (1983). In *Muscle and Nonmuscle Motility* (Stracher, A., ed.), vol. 1, pp. 151–216. Academic Press, New York.
Oosawa, F. & Asakura, S. (1975). *Thermodynamics of the Polymerization of Protein*, Academic Press, New York.
Oosawa, F., Fujime, S., Ishiwata, S. & Mihashi, K. (1973). *Cold Spring Harbor Symp. Quant. Biol.* **37**, 277–285.
Rigler, R. & Ehrenberg, H. (1973). *Quart. Rev. Biophys.* **6**, 139–199.
Schurr, J. M. (1984). *Chem. Phys.* **84**, 71–96.
Shibata, J. H., Wilcoxon, J., Schurr, J. M. & Knauf, V. (1984). *Biochemistry*, **23**, 1188–1194.
Squire, J. (1981). *The Structural Basis of Muscular Contraction*, chap. 5. Plenum Press, New York.
Tajima, Y., Kamiya, K. & Seto, T. (1983). *Biophys. J.* **43**, 335–343.
Thomas, D. D., Seidel, J. C. & Gergely, J. (1979). *J. Mol. Biol.* **132**, 257–273.
Vibert, P. J., Haselgrove, J. C., Lowy, J. & Poulsen, F. R. (1972). *J. Mol. Biol.* **71**, 757–767.
Wahl, Ph., Mihashi, K. & Auchet, J.-P. (1975). *FEBS Letters*, **8**, 164–167.
Wakabayashi, T., Huxley, H. E., Amos, L. A. & Klug, A. (1975). *J. Mol. Biol.* **93**, 477–496.
Yanagida, T. & Oosawa, F. (1978). *J. Mol. Biol.* **126**, 507–524.
Yanagida, T., Nakase, M., Nishiyama, K. & Oosawa, F. (1984). *Nature (London)*, **307**, 58–60.
Yoshimura, H. & Mihashi, K. (1982). *J. Biochem.* **92**, 497–508.

Edited by C. R. Cantor